Cell Reports, Volume *43*

Supplemental information

Mapping of susceptibility loci for Ebola virus pathogenesis in mice

Alexandra Schäfer, Andrea Marzi, Wakako Furuyama, Nicholas J. Catanzaro, Cameron Nguyen, Elaine Haddock, Friederike Feldmann, Kimberly Meade-White, Tina Thomas, Miranda L. Hubbard, Kendra L. Gully, Sarah R. Leist, Pablo Hock, Timothy A. Bell, Gabriela E. De la Cruz, Bentley R. Midkiff, David R. Martinez, Ginger D. Shaw, Darla R. Miller, Michael J. Vernon, Rachel L. Graham, Dale O. Cowley, Stephanie A. Montgomery, Klaus Schughart, Fernando Pardo Manuel de Villena, Gregory K. Wilkerson, Martin T. Ferris, Heinz Feldmann, and Ralph S. Baric

Supplemental Figures

Figure S1. Different disease severity of CC011 and CC074 after MA-EBOV infection. A. Gross pathology scores in the liver of CC011 and CC074 on a scale from 0 (no change) to 4 (100% changed) (n=16 for each strain, both sexes). **B.** Representative images (20x and 40x, respectively) of the fibrinogen, cleaved caspase 3 (apoptosis), and CD31 (endothelial marker) immunostained liver sections utilized for the histological assessment of differences between CC011 and CC074 at 3 dpi and 6 dpi; scale bars indicate 50μm. Immunostaining for fibrinogen was most often associated with leukocytes (inflammation) and sinusoidal endothelium. Immunostaining for cleaved caspase 3 (apoptosis) was most often associated with hepatocytes and leukocytes in nearly equal numbers except for the CC074 6 dpi mice where leukocyte immunostaining predominated. Also, cleaved caspase 3 immunostaining of the vascular endothelium occurred less frequently in the CC011 as compared to CC074 livers. Immunostaining for CD31 (endothelial marker) at 6 dpi was excessive in sinusoids for both CC strains.

Figure S2. Weight loss and viral load of CC011xCC074-F2 mice. Eight- to 10-week-old CC011xCC074-F2 mice (n=236; 123 females, 113 males) were infected with 100 ffu MA-EBOV i.p. Weight loss for **A.** male and **B.** female CC011xCC074-F2 mice over the time of infection, bold lines indicate mean weights of CC011 (black) and CC074 (red) parental strains, respectively. **C.** Viral load in the liver for CC011xCC074-F2 on 6 dpi. **D.** Correlation analysis of viral load in liver (ffu equivalent/mg tissue) and weight loss for CC011xCC074-F2 on 6 dpi.

Figure S3. Identification of a QTL on Chr8 for viral load in the blood and the liver. The 8- to 10-week-old CC011xCC074-F2 mice (n=236; 123 females, 113 males) were generated and infected with 100 ffu MA-EBOV i.p. and followed for 6 days for weight loss and mortality. **A.** Viral load in the blood at 6 dpi (ffu equivanlents/ml). **B.** QTL map for the viral load in the blood on 6

dpi. **C.** Correlation analysis of viral load in blood and weight loss for CC011xCC074-F2 on 6 dpi. **D.** Viral load in the liver at 6 dpi (ffu equivanlents/mg). **E.** QTL map for viral load in the liver on 6 dpi. LOD = log10 likelihood ratio; dotted line indicates the genome-wide p=0.05 significance threshold.

Figure S4. Different EVD-like disease of *Trim*$^{-/-}$ and *Trim*$^{+/+}$ after MA-EBOV infection. A. Left panel: The zinc finger residues of the WT TRIM5 B-box 2 are highlighted in magenta. The histidine residue of interest is shown in stick representation. Middle panel: The zinc finger residues of the mutated B-box 2 are highlighted in orange. Mutation of the penultimate histidine to glutamine rotates the amino acid out of proximity to the zinc-binding domain. Right panel: Merged image of WT and mutant zinc fingers. To model the structural effects of the zinc finger mutation in TRIM5, homology modeling was performed using the published TRIM5 B-box 2 sequence (PDB: 2YRG). The structure of the sequence was modeled using the Phyre2 Protein Fold Recognition Server (http://sbg.bio.ic.ac.uk). The model chosen for alignment had 99.2% confidence and 79% identity. The downloaded model was then overlaid on the published structure in PyMOL (The PyMOL Molecular Graphics System, Version 2.0 Schrödinger, LLC.), and the mutant residue in the zinc finger was highlighted. **B.** Design for engineering of the Trim-/- mice. **C.** *Trim*$^{-/-}$ animals were detected by PCR, a ~593 bp band for the *Trim*$^{-/-}$ allele and a 466 bp band for the *Trim* wild-type allele (*Trim*$^{+/+}$), double-band indicates heterozygosity. **D.** Expression of *Trim* genes from *Trim5* locus as validated by whole genome RNA-seq. **E.** Weight loss for *Trim*$^{-/-}$ and *Trim*$^{+/+}$ mice used for immunohistological evaluation and gene expression profiling. **F.** Distribution of gross pathology phenotypes for *Trim*$^{-/-}$ mice and *Trim*$^{+/+}$ mice (from E.). **G.** Representative images (20x and 40x, respectively) of the fibrinogen, cleaved caspase 3 (apoptosis), and CD31 (endothelial marker) immunostained liver sections utilized for the histological assessment of differences between *Trim*$^{-/-}$ mice and *Trim*$^{+/+}$ mice at 3 dpi and 6 dpi; scale bars indicate 50μm Immunostaining for fibrinogen was most often associated with

leukocytes (inflammation) and sinusoidal endothelium. Immunostaining for cleaved caspase 3 (apoptosis) was most often associated with hepatocytes and leukocytes at 3 dpi and included some vascular endothelium staining at 6 dpi. Immunostaining for CD31 (endothelial marker) at 6 dpi was excessive in sinusoids for *Trim*$^{-/-}$ mice and *Trim*$^{+/+}$ mice. Data were analyzed using Mann-Whitney test (weight loss).

Figure S5. Differentially-expressed gene signatures indicate upregulated inflammatory and cytokine responses and a downreguation of metabolic processes in the liver of CC011xCC074-F2 mice with severe EVD-like disease. The 8-10-week-old CC011xCC074-F2 mice (n=236; 123 females, 113 males) were generated and infected with 100 ffu MA-EBOV i.p. and followed for 6 days for weight loss and mortality. CC011xCC074-F2 mice were stratified based on their weight loss and the top 15 mice at the extreme ends of bodyweight loss and total RNA from liver tissues subjected to RNA-seq. **A.** Percent starting body weight of high weight loss (HWL), the low weight loss (LWL), and the uninfected (UI, n=9) groups. **B.** Viral load in the liver for CC011xCC074-F2 mice on 6 dpi. **C.** Distribution of gross pathology phenotypes for CC011xCC074-F2 mice from the high weight loss group (HWL), and the low weight loss group (LWL). Gross pathology scores on a scale from 0 (no change) to 4 (100% changed). **D.** Heatmap of the top 5 ranked genes in the top 10 significantly enriched pathways of infected groups (HWL and LWL) compared to the UI group (< 1.5 Log_2 fold over mock; $p < 0.05$); shown are the average expression levels for each gene for each group, UI=9 mice, LWL=15 mice, and HLW=15 mice, respectively. Data were analyzed using Mann-Whitney test (liver titer).

Table S1. Scoring of histopathological findings in CC011, CC074, Trim$^{-/-}$, and Trim$^{+/+}$ mice.

Table S2. SNPs in CC011 and CC074 within the *QES1* and *QES2* loci.

Table S3. Genes that are differentially expressed on 3dpi and 6dpi in CC011, CC074, *Trim*$^{-/-}$, *Trim*$^{+/+}$, and CC011xCC074-F2 mice (6dpi only) (<1.5 Log_2 over mock, $p < 0.05$).

Table S4. Gene of the top five ranked genes in the top 20 significantly enriched pathways of infected groups CC011 and CC074 (3dpi and 6dpi) compared to their respective uninfected control group.

Table S5. Gene of the top five ranked genes in the top 20 significantly enriched pathways of infected groups (HWL and LWL) compared to the UI group.

Table S6. Gene of the top five ranked genes in the top 20 significantly enriched pathways of infected groups *Trim*$^{-/-}$ and *Trim*$^{+/+}$ (6dpi) compared to their respective uninfected control group.

TableS7. Key genes with significant expression changes during the development of liver disease during EBOV infection.

Figure S1

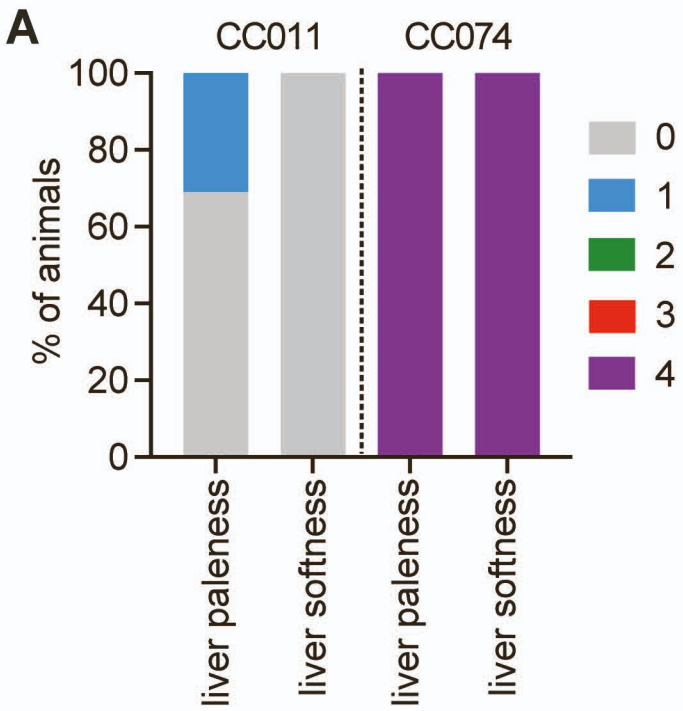
A
CC011
CC074
100
80
60
40
20
0
% of animals
liver paleness
liver softness
liver paleness
liver softness
0
1
2
3
4

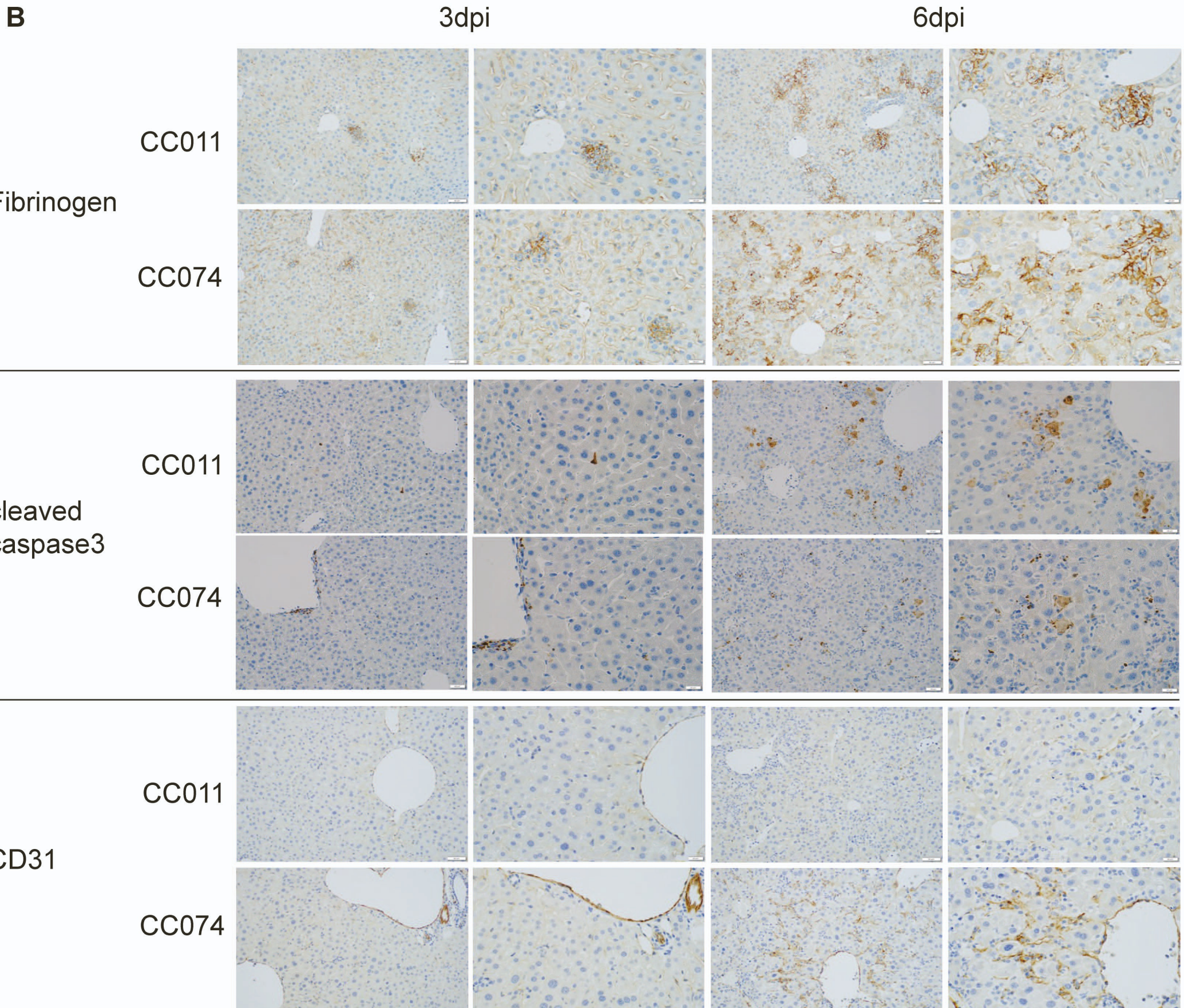
B
3dpi
6dpi
CC011
Fibrinogen
CC074
CC011
cleaved caspase3
CC074
CC011
CD31
CC074

Figure S2

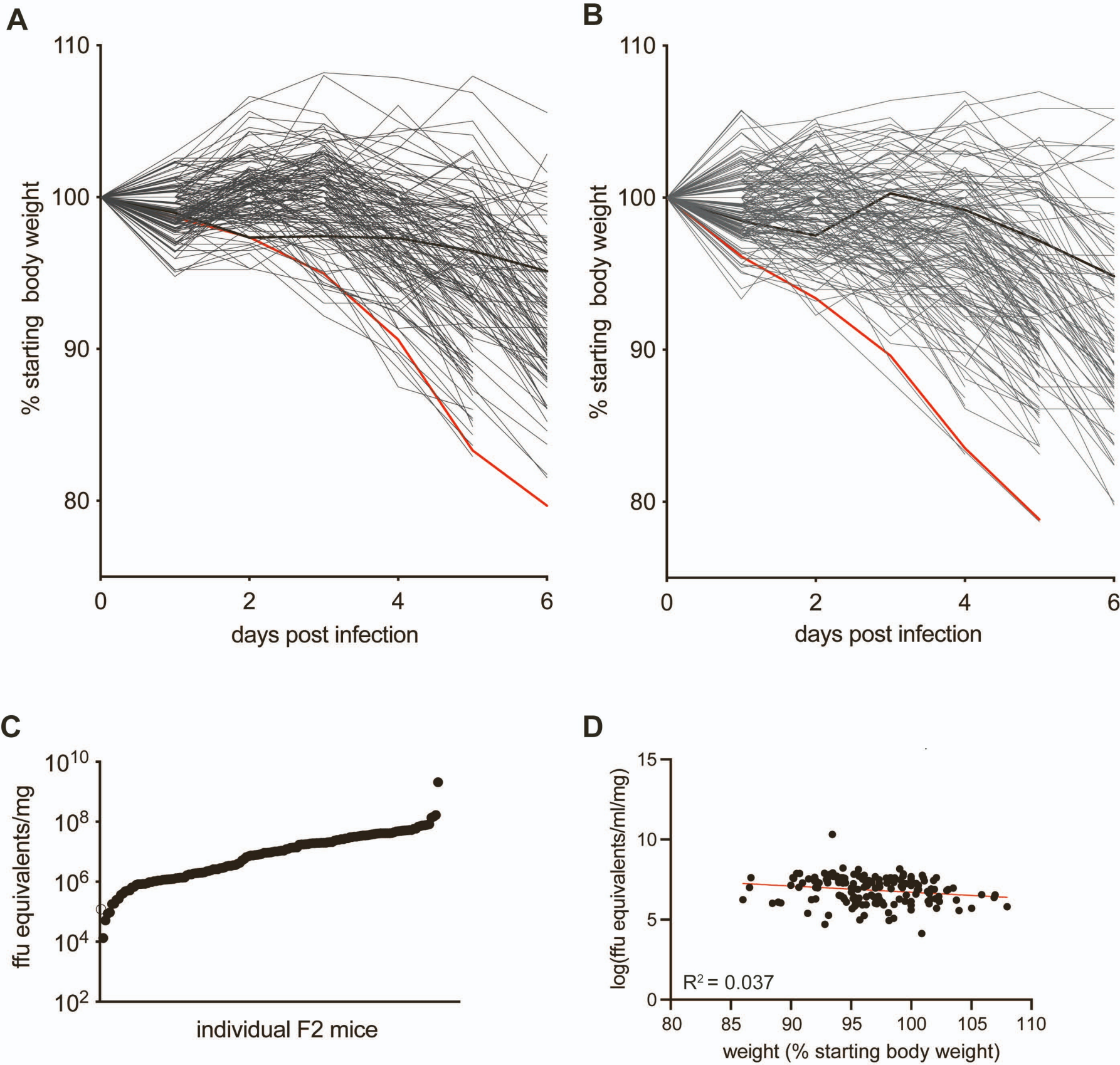
A
B
110
100
90
80
% starting body weight
0
2
4
6
days post infection
C
D
10^{10}
10^{8}
10^{6}
10^{4}
10^{2}
ffu equivalents/mg
individual F2 mice
15
10
5
0
log(ffu equivalents/ml/mg)
R^2 = 0.037
80
85
90
95
100
105
110
weight (% starting body weight)

Figure S3

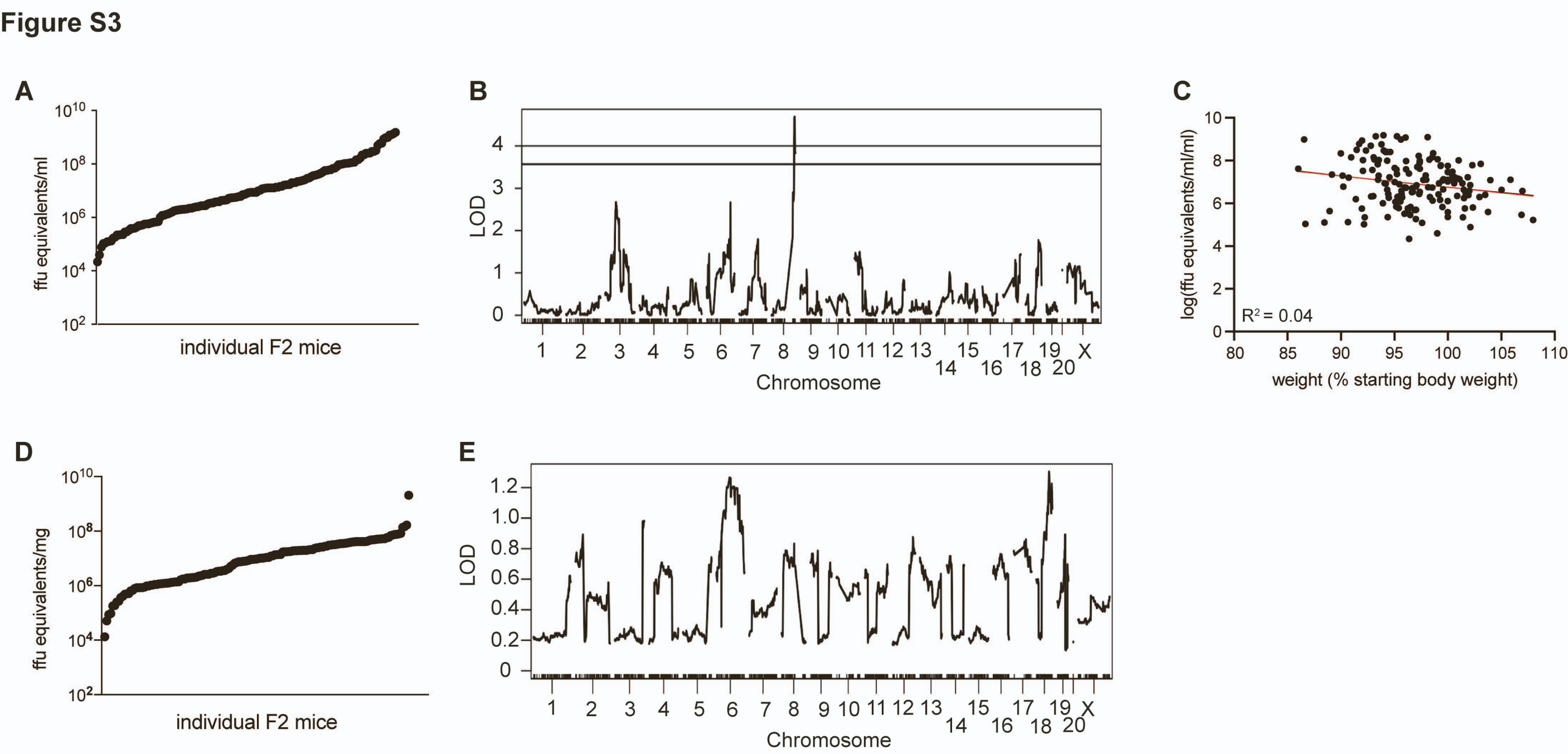
A
ffu equivalents/ml
individual F2 mice
B
LOD
Chromosome
C
log(ffu equivalents/ml/ml)
weight (% starting body weight)
R² = 0.04
D
ffu equivalents/mg
individual F2 mice
E
LOD
Chromosome

Figure S4

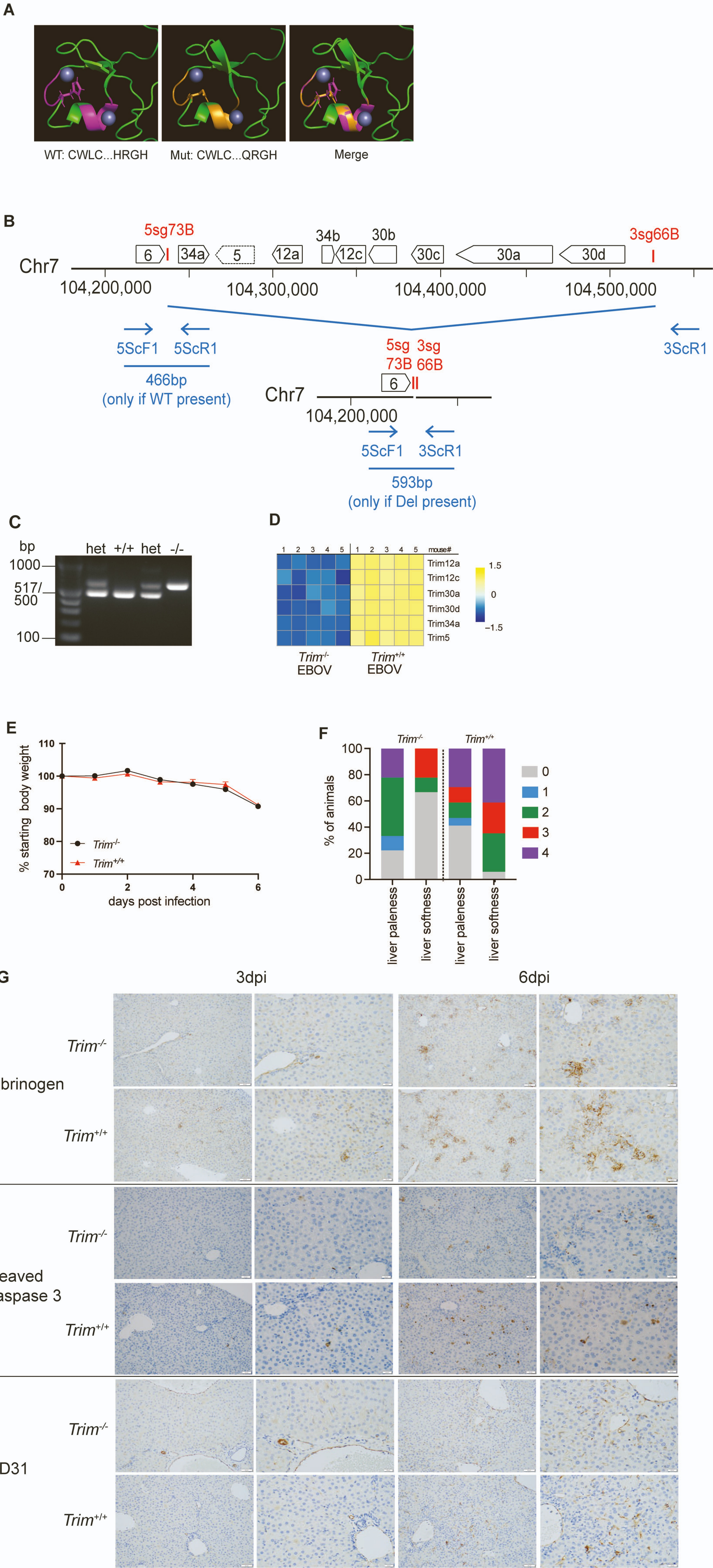
A
WT: CWLC...HRGH
Mut: CWLC...QRGH
Merge
B
5sg73B
3sg66B
6
34a
5
12a
34b
12c
30b
30c
30a
30d
Chr7
104,200,000
104,300,000
104,400,000
104,500,000
5ScF1
5ScR1
466bp
(only if WT present)
3ScR1
5sg
73B
3sg
66B
6
Chr7
104,200,000
5ScF1
3ScR1
593bp
(only if Del present)
C
bp
het
+/+
het
-/-
1000
517/
500
100
D
1 2 3 4 5 1 2 3 4 5
mouse#
Trim12a
Trim12c
Trim30a
Trim30d
Trim34a
Trim5
1.5
0
−1.5
Trim-/-
EBOV
Trim+/+
EBOV
E
% starting body weight
110
100
90
80
70
0
2
4
6
days post infection
Trim-/-
Trim+/+
F
Trim-/-
Trim+/+
% of animals
100
80
60
40
20
0
0
1
2
3
4
liver paleness
liver softness
liver paleness
liver softness
G
3dpi
6dpi
Trim-/-
Fibrinogen
Trim+/+
Trim-/-
cleaved
caspase 3
Trim+/+
Trim-/-
CD31
Trim+/+

Figure S5

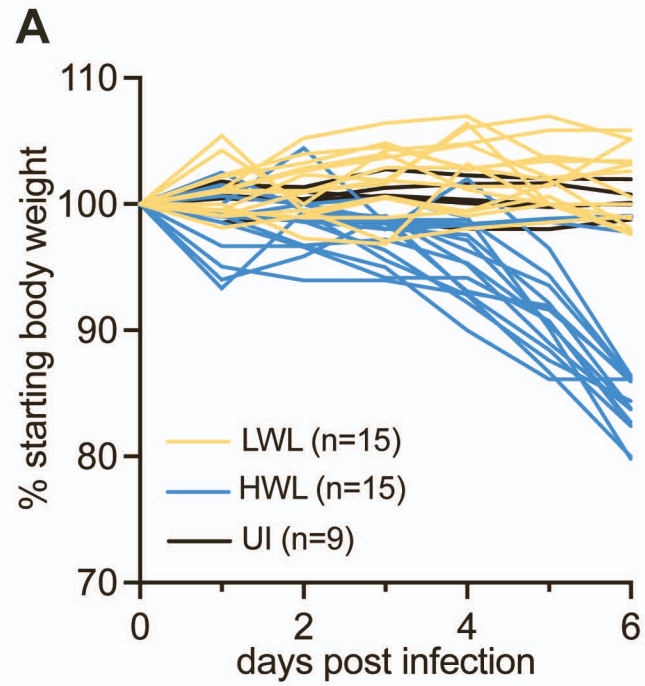
A
110
100
90
80
70
% starting body weight
0
2
4
6
days post infection
LWL (n=15)
HWL (n=15)
UI (n=9)

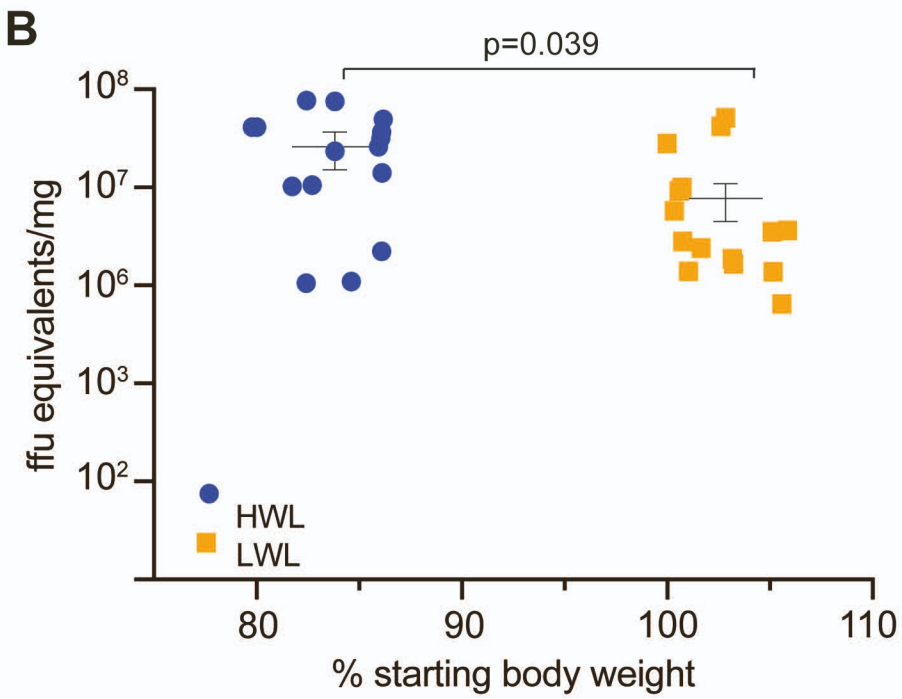
B
p=0.039
10^8
10^7
10^6
10^3
10^2
ffu equivalents/mg
HWL
LWL
80
90
100
110
% starting body weight

C
LWL (n=15)
HWL (n=15)
100
80
60
40
20
0
% of animals
0
1
2
3
4
liver paleness
liver softness
liver paleness
liver softness

D
TNFα Signaling via NFκB
Bile Acid Metabolism
Epithelial Mesenchymal Transition
Inflammatory Response
Hypoxia
Xenobiotic Metabolism
E2F Targets
G2M Checkpoint
Kras Signaling
Fatty Acid Metabolism
UI
LWL
HWL
1
0.5
0
−0.5
−1

Table S3

Comparison	**Up**	**down**	
CC011 mock vs CC011 3dpi	966	2114	Figure 5
CC011 mock vs CC011 6dpi	1205	2243	
CC074 mock vs CC074 3dpi	1860	3051	
CC074 mock vs CC074 6dpi	436	435	
CC011 3dpi vs CC74 3dpi	435	594	
CC011 6dpi vs CC074 6dpi	477	180	
$Trim^{-/-}$ mock vs $Trim^{-/-}$ 3dpi	363	611	Figure 6
$Trim^{-/-}$ mock vs $Trim^{-/-}$ 6dpi	962	1325	
$Trim^{+/+}$ mock vs $Trim^{+/+}$ 3dpi	215	570	
$Trim^{+/+}$ mock vs $Trim^{+/+}$ 6dpi	1481	1638	
$Trim^{+/+}$ 3dpi vs $Trim^{-/-}$ 3dpi	8	2	
$Trim^{+/+}$ 6dpi vs $Trim^{-/-}$ 6dpi	134	56	
LWL 6dpi vs HWL 6dpi	210	451	Figure S5

Table S7

	3dpi			6dpi		
Gene	Trim+/+	Trim-/-	p	Trim+/+	Trim-/-	p
Vegfa	8.41 +/- 0.38	9.32 +/- 0.85	0.0556	6.6 +/- 0.19	7.05 +/- 0.29	**0.0317**
Itgb8	0.58 +/- 0.42	1.14 +/- 0.32	0.0952	2.13 +/- 0.29	2.46 +/- 0.04	**0.0317**
Mmp2	0.26 +/- 0.46	1.13 +/- 0.41	**0.0317**	1.59 +/- 0.43	2.44 +/- 0.27	**0.0079**
F7	7.12 +/- 0.11	6.77 +/-/ 0.11	**0.0079**	5.61 +/- 0.14	5.87 +/- 0.16	**0.0317**
Cdh	5.83 +/- 0.27	4.99+/- 0.41	**0.0079**	5.14 +/- 0.26	6.02 +/- 0.47	**0.0079**
Cyp39a1	1.49 +/- 0.94	2.78 +/- 1.13	**0.0317**	2.44 +/- 0.41	1.72 +/- 0.55	0.0952
Agxt	7.92 +/- 0.26	6.74 +/- 0.8	**0.0079**	5.49 +/- 0.48	6.28 +/- 0.62	0.0556
Alb	15.03 +/- 0.6	14.31 +/- 1.04	0.2222	12.3 +/- 0.54	13.78 +/- 0.16	**0.0079**
Ang	9.41 +/- 0.22	8.44 +/- 0.51	**0.0317**	7.4 +/- 0.36	8.3 +/- 0.19	**0.0079**
Apoa2	11.02 +/- 0.5	10.53 +/- 0.73	0.2222	7.95 +/- 0.36	9.27 +/- 0.28	**0.0079**
Apoc1	10.84 +/- 0.39	10.06 +/- 0.77	0.1508	8.96 +/- 0.34	10.11 +/- 0.2	**0.0079**
Apob	13.66 +/- 0.16	13.0 +/- 0.46	**0.0317**	13.00 +/- 0.46	13.66 +/- 0.16	**0.0079**
Aldh7a1	7.73 +/- 0.28	7.35 +/- 0.46	0.0952	6.15 +/- 0.32	6.87 +/- 0.29	**0.0079**
Adipor	8.16 +/- 0.31	7.98 +/- 0.78	0.5476	7.04 +/- 0.27	7.49 +/- 0.2	**0.0317**
C4bp	9.14 +/- 0.23	8.29 +/- 0.56	**0.0159**	8.54 +/- 0.17	9.44 +/- 0.14	**0.0079**
C1qbp	5.34 +/- 0.07	4.58 +/- 0.76	0.1508	4.2 +/- 0.3	5.15 +/- 0.14	**0.0079**
Cers4	2.65 +/- 0.17	3.53 +/- 0.56	**0.0317**	2.86 +/- 0.25	2.64 +/- 0.46	0.4206
Ces2a	6.55 +/- 0.43	6.26 +/- 0.66	**0.4206**	3.52 +/- 0.34	4.72 +/- 0.5	**0.0079**
Crp	9.3 +/- 0.41	8.12 +/- 0.67	**0.0317**	8.4 +/- 0.48	7.44 +/- 0.31	**0.0159**
Dhfr	4.16 +/- 0.44	3.53 +/- 0.84	0.2222	3.03 +/- 0.16	3.65 +/- 0.28	**0.0079**
F13b	6.84 +/- 0.62	6.06 +/- 0.83	0.1508	4.62 +/- 0.4	5.94 +/- 0.42	**0.0079**
Fgb	11.53 +/- 0.77	12.33 +/- 0.25	0.0952	11.51 +/- 0.48	12.66 +/- 0.12	**0.0079**

Fgg	11.87 +/- 0.26	11.18 +/- 0.74	0.2222	10.96 +/- 0.52	12.17 +/- 0.16	**0.0079**
Serpina1a	11.15 +/- 0.28	10.44 +/- 0.6	0.0952	9.66 +/- 0.32	10.5 +/- 0.21	**0.0079**
Serpina7	6.2 +/- 0.45	4.3 +/- 1.38	0.0952	5.84 +/- 0.22	6.75 +/- 0.39	**0.0159**
Itih1	9.65 +/- 0.08	9.28 +/- 0.16	**0.0079**	8.57 +/- 0.28	9.02 +/- 0.16	**0.0159**
Itih3	10.45 +/- 0.3	8.77 +/- 1.15	**0.0317**	9.27 +/- 0.45	10.59 +/- 0.17	**0.0079**
Pdk4	2.66 +/- 0.53	4.39 +/- 0.98	**0.0159**	4.75 +/- 0.85	4.59 +/- 0.63	0.8413
Pdia6	3.76 +/- 0.43	3.44 +/- 0.63	0.4206	3.53 +/- 0.15	3.9 +/- 0.26	**0.0317**
Ttr	11.34 +/- 0.48	10.55 +/- 0.85	0.2222	9.02 +/- 0.37	10.43 +/- 0.43	**0.0079**
Serpinc1	10.67 +/- 0.15	10.37 +/- 0.36	0.1508	8.65 +/- 0.17	9.62 +/- 0.19	0.1508
Saa1	12.98 +/- 1.74	9.74 +/- 3.28	0.0952	11.4 +/- 0.09	12.27 +/- 0.19	**0.0079**
Saa2	12.09 +/- 2.24	8.36 +/- 3.45	0.0556	10.58 +/- 0.08	11.45 +/- 0.19	**0.0079**
Lipc	6.1 +/- 0.61	4.62 +/- 1.08	**0.0159**	3.76 +/- 0.24	4.71 +/- 0.48	**0.0159**
Lcat	8.65 +/- 0.08	7.72 +/- 0.47	**0.0079**	7.31 +/- 0.29	8.46 +/- 0.25	**0.0079**
Sult2a1	4.94 +/- 1.21	5.63 +/- 1.28	0.6905	1.91 +/- 1.68	3.77 +/- 0.71	**0.0159**
Hamp	10.39 +/- 0.48	9.48 +/- 0.59	0.0556	8.78 +/- 0.38	10.06 +/- 0.16	**0.0079**
Hyal3	0.44 +/- 0.32	0.76 +/- 0.22	0.1508	0.55 +/- 0.14	0.15 +/- 0.06	**0.0079**
Hpn	9.01 +/- 0.06	8.53 +/- 0.26	**0.0159**	7.15 +/- 0.31	7.3 +/- 0.16	0.6905
Orm1	11.41 +/- 0.88	9.1 +/-1.68	0.0556	10.04 +/- 0.22	11.43 +/- 0.2	**0.0079**
Rhno1	2.49 +/- 0.3	2.49 +/- 0.27	>0.9999	3.55 +/- 0.14	3.01 +/- 0.29	**0.0159**
Mrlp55	3.51 +/- 0.17	2.92 +/- 0.4	**0.0159**	2.52 +/- 0.19	3.22 +/- 0.18	**0.0079**
Tek	2.92 +/- 0.46	3.22 +/- 0.73	0.8413	1.53 +/- 0.29	2.0 +/- 0.32	**0.0317**